



HAL
open science

Low-Temperature Transport Properties of Bi-Substituted β -As₂Te₃ Compounds

Jean-Baptiste Vaney, Julie Carreaud, Gaëlle Delaizir, Cédric Morin, Judith Monnier, Eric Alleno, Andrea Piarristeguy, Annie Pradel, Antonio P. Goncalves, Elsa B. Lopes, et al.

► **To cite this version:**

Jean-Baptiste Vaney, Julie Carreaud, Gaëlle Delaizir, Cédric Morin, Judith Monnier, et al.. Low-Temperature Transport Properties of Bi-Substituted β -As₂Te₃ Compounds. *Journal of Electronic Materials*, 2016, 45 (3), pp.1786-1791. 10.1007/s11664-015-4227-1 . hal-01279971

HAL Id: hal-01279971

<https://hal.science/hal-01279971>

Submitted on 9 Mar 2023

HAL is a multi-disciplinary open access archive for the deposit and dissemination of scientific research documents, whether they are published or not. The documents may come from teaching and research institutions in France or abroad, or from public or private research centers.

L'archive ouverte pluridisciplinaire **HAL**, est destinée au dépôt et à la diffusion de documents scientifiques de niveau recherche, publiés ou non, émanant des établissements d'enseignement et de recherche français ou étrangers, des laboratoires publics ou privés.

Title:

Low temperature transport properties of Bi substituted β -As₂Te₃ compounds

Authors

J-B. Vaney^{1,2}, J. Carreaud², G.Delaizir², C. Morin³, J. Monnier³, E. Alleno³, A. Piarristeguy⁴, A.Pradel⁴, A.P. Gonçalves⁵, E.B. Lopes⁵, C.Candolfi¹, A.Dauscher¹, B.Lenoir¹

Affiliations

¹*Institut Jean Lamour (IJL), UMR 7198 CNRS-Université de Lorraine, France*

²*SPCTS, Université de Limoges UMR CNRS 7315, France*

³*Institut de Chimie et des Matériaux de Paris Est (ICMPE), UMR 7182 CNRS, CMTR, Thiais, France*

⁴*Institut Charles Gerhardt (ICG), UMR 5253 CNRS-Université Montpellier 2, France*

⁵*C2TN Instituto Superior Técnico, Universidade Técnica de Lisboa, P-2695-066 Bobadela LRS, Portugal*

Abstract:

β -As₂Te₃ belongs to the family of Bi₂Te₃-based alloys, a well-known class of efficient thermoelectric materials around room temperature. As₂Te₃ exists in two allotropic configurations: α - and β -As₂Te₃, of which only the latter crystallizes in the same rhombohedral structure as Bi₂Te₃. Herein, we report on the substitution of Bi for As in the system As_{2-x}Bi_xTe₃ with $x = 0.0, 0.015, 0.025$ and 0.035 . These samples have been characterized by X-ray diffraction and scanning electron microscopy. The transport properties have been measured at low temperatures (5 – 300 K) in both directions, parallel and perpendicular to the pressing direction. The results are compared to those obtained in a previous study on samples substituted by Sn. Compared to Sn, Bi allows for a clear decrease in electrical resistivity while maintaining the thermal conductivity below 1 W/m.K over the whole temperature range. As a result, a comparable peak ZT value near 0.2 was obtained at room temperature

Introduction

In the current context of environmental concerns, energy harvesting has become a central focus in materials science research. Among all the technologies under scrutiny and development, thermoelectricity might play a

role due to its numerous advantages such as the absence of gaseous emission, vibration-free character and versatility. However, for decades, the performance and efficiency of thermoelectric (TE) materials has been limited, confining them to niche applications and markets. Near room temperature, Peltier coolers are used as solid-state heat pumps for electronic device cooling for example [1].

The thermoelectric performance of TE materials is quantitatively described by the dimensionless figure of merit ZT defined as $ZT = \alpha^2 T / \rho \lambda$, where α is the Seebeck coefficient or thermopower, T is the absolute temperature, ρ is the electrical resistivity and λ is the total thermal conductivity. Achieving high ZT on a broad temperature range still represents one of the most challenging aspect in thermoelectricity [2-3]. The ternary or quaternary compounds based on $A_2^V B_3^{VI}$ ($A = \text{Bi}$ or Sb and $B = \text{Te}$ or Se) compounds remain the most efficient thermoelectric materials to date, for applications close to room-temperature. When properly optimized, both p -type and n -type compounds show ZT values close to unity near 300K.

$\beta\text{-As}_2\text{Te}_3$ is one of the two allotropic forms of As_2Te_3 (together with $\alpha\text{-As}_2\text{Te}_3$, monoclinic, space group $C2/m$) and, as Bi_2Te_3 , belongs to the family of compounds crystallizing in the rhombohedral space group $R\bar{3}m$. $\beta\text{-As}_2\text{Te}_3$ has been reported to be a high-pressure phase, with a transition from α - to $\beta\text{-As}_2\text{Te}_3$ near 7 GPa [4]. Further studies unveiled that quenching could be an efficient method to produce these phases at ambient pressure [5-6] although they were not extensively studied from the thermoelectric point of view so far. Recently, we demonstrated that $\beta\text{-As}_2\text{Te}_3$ could be stabilized under ambient conditions and that the carrier concentration could be tuned by alloying with Sn, leading to enhanced thermoelectric performance ($ZT \sim 0.6$ at 423K) [7].

In this article, we report on the effect of the substitution of Bi for As on the thermoelectric properties of $\beta\text{-As}_2\text{Te}_3$ at low temperatures (5 – 300 K). We evidence that Bi is another element that might lead to interesting thermoelectric properties in p -type $\beta\text{-As}_{2-x}\text{Bi}_x\text{Te}_3$ (up to $x = 0.035$) above room-temperature.

Experimental

All $\beta\text{-As}_{2-x}\text{Bi}_x\text{Te}_3$ ($x = 0.0, 0.015, 0.025, 0.035$) samples were prepared by direct reaction of stoichiometric amounts of pure elements (As (Goodfellow, 99.99%, shots), Te (5N+, 99.999%, shots) and Bi (Strem Chemicals, 99.9999%, shots)) sealed under secondary vacuum in quartz tubes. The tubes were heated slowly up to 923 K at a rate of 10 K min^{-1} , dwelt at this temperature for 2 hours and finally quenched in icy water. The resulting ingots were hand-ground into micron-sized powders and cold-pressed into 10 mm diameter cylindrical pellets under a pressure of 750 MPa. Remarkably, all the obtained ingots showed an experimental density higher than 95% of

the theoretical density situation reminiscent to what is also observed in $(\text{Bi,Sb})_2(\text{Se,Te})_3$ compounds [1]. Noteworthy, for this phase, sintering techniques such as hot-pressing or spark plasma sintering could not be used as the required temperatures trigger the phase transition of β - to α - As_2Te_3 that sets in at X K.

The crystal structure was determined by powder X-ray diffraction (PXRD) at 300 K with a Bruker D8 Advance instrument using monochromated $\text{CuK}\alpha_1$ radiation. The chemical homogeneity of the samples was checked by scanning electron microscopy (SEM) and energy dispersive x-ray spectroscopy (EDXS) using a Quanta FEG (FEI).

The thermoelectric properties were measured simultaneously between 5 and 300 K on parallelepiped-shaped samples cut with a diamond wire-saw (typical dimensions of $2 \times 3 \times 7 \text{ mm}^3$) using the thermal transport option of a physical property measurement system (PPMS, Quantum Design). Fine Cu wires were brazed to the samples ensuring good electrical and thermal contacts, in a four collinear contacts set-up. Owing to the anisotropic crystal structure of the studied compounds, the transport properties were measured on samples cut both parallel and perpendicular to the pressing direction. The Hall coefficient R_H was measured at 300 K on the perpendicular samples (same as used for TTO option) with the ac transport option of the PPMS. The magnetic field was swept between -0.5 and +0.5 T. The hole concentration p and Hall mobility μ_H were estimated from $p = 1 / eR_H$ and $\mu_H = R_H / \rho$.

Results and discussion

Figure 1 presents the PXRD patterns (Fig. 1-A) obtained for the illustrative $x = 0.025$ sample (all diffraction patterns being very similar) together with the evolution of the lattice parameter (Fig. 1-B) and a sketch of the crystal structure of this compound (Fig.1-C). All reflections can be indexed in the $R\bar{3}m$ space group with an additional peak ascribed to non quantifiable AsTe impurities ($Fm\bar{3}m$, $a = 5.778 \text{ \AA}$) existing for all compositions. Due to the anisotropy of the crystal structure, all the samples show a preferred orientation, resulting in a slight renormalization of the relative intensities of the Bragg peaks. Rietveld refinements against the PXRD patterns lead to good fits, allowing a precise determination of the hexagonal lattice parameters of $\beta\text{-As}_{2-x}\text{Bi}_x\text{Te}_3$ (Figure 1-B). The values inferred for the binary compound are in agreement with literature data ($a = 4.0473 \text{ \AA}$ and $c = 29.5018 \text{ \AA}$). The unit cell volume expands monotonically with increasing the Bi content up to $x = 0.035$ as a result of a simultaneous increase along the a and c axes. The expansion is however not linear and hints at a

saturation threshold at higher x . These data are consistent with the effective insertion of Bi into the crystal structure of β -As₂Te₃.

Scanning electron microscopy (SEM) and X-Ray mapping further revealed an overall homogeneous distribution of the different elements in the samples regardless of the composition, as displayed for the $x = 0.035$ specimen in Figure 2.

The temperature dependences of ρ and α measured parallel and perpendicular to the pressing direction are displayed in Figures 3-A and 3-B respectively. The values of ρ exhibit a noticeable anisotropy with a twofold increase in ρ in the parallel direction with respect to the perpendicular direction. Except for the binary compound, which displays a slightly lower electrical resistivity than the other compounds, no clear trend with the Bi content can be observed. This conclusion holds true for the anisotropy that hardly evolve with increasing x . However, a clear change in the temperature evolution can be observed around 175 K for each sample. This change reflects a structural transformation of β -As₂Te₃ into an analogous monoclinic structure β' -As₂Te₃ (Morin et al. *to be published*). The values of α are positive, indicating transport dominated by holes, with an almost linear increase for each sample along the whole temperature range. At 300 K, the substitution of Bi for As leads to a slight increase in α from 103 $\mu\text{V}\cdot\text{K}^{-1}$ for $x = 0.0$ to 117 $\mu\text{V}\cdot\text{K}^{-1}$ for $x = 0.025$ and 0.035 . The change in the slope observed at 175 K is consistent with that observed in the ρ data and is thus ascribed to the structural transition $\beta \rightarrow \beta'$. Anisotropy is observed between the two measuring directions, fading out for $x = 0.035$. Compared to the effects of As/Sn substitution where a strong increase in both the electrical resistivity and the thermopower is observed up to an Sn content of 0.035, these two properties hardly evolve upon isoelectronic substitution of Bi for As at 300K.

Table 1 presents the Hall carrier concentration (p) and Hall mobility (μ_{H}) measured at 300 K for $x = 0, 0.015$ and 0.025 and 0.035 . Only a very subtle evolution can be observed between the three Bi-substituted samples while the value of p for the non-substituted compound lies at slightly higher values, below 10^{20} cm^{-3} . Mobility values at 300K firstly increase from the initial value of $\sim 49 \text{ cm}^2\cdot\text{V}^{-1}\cdot\text{s}^{-1}$ for the nominal compound to the very high value of ~ 81 for $x = 0.015$. For upper x , the electronic mobility constantly decreases down to ~ 58 for $x = 0.035$.

Figure 4-A shows the temperature dependence of the total thermal conductivity λ . The anisotropic behavior is similar to that displayed by the electrical resistivity data, even though being opposite, with a thermal conductivity in the parallel direction considerably lower than in the perpendicular direction. Compared to the $\text{As}_{2-x}\text{Sn}_x\text{Te}_3$ compounds, the decrease in the λ values due to Bi substitution is less marked. Given the monotonic increase in electrical resistivity upon Sn substitution in contrast to the moderate evolution observed here, the electronic contribution to λ is considerably lowered in the former with respect to the latter, resulting in a stronger decrease in λ when substituting Sn for As. The values range between 0.7 and 1 $\text{W}\cdot\text{m}^{-1}\cdot\text{K}^{-1}$ in the parallel direction while decreasing around 0.5 $\text{W}\cdot\text{m}^{-1}\cdot\text{K}^{-1}$ for the Sn-substituted compounds at 300 K [7]. Figure 4-B shows the lattice thermal conductivity as a function of the temperature calculated by subtracting the electronic contribution estimated by the Wiedemann-Franz law ($\lambda_e = TL/\rho$, where $L = 2.44 \times 10^{-8} \text{ W } \Omega \text{ K}^{-2}$ is the Lorenz number). The observed lattice thermal conductivities range from 0.8 $\text{W}/(\text{m K})$ to slightly above 0.4 $\text{W}/(\text{m K})$ at 300 K, bearing in mind that due to the experimental setup, room-temperature thermal conductivity is always slightly overestimated (due to difficulties in estimating radiation losses in a direct measurement).

A remarkable feature rarely observed in the Bi_2Te_3 family of compounds is the absence of a dielectric peak at low temperatures, mimicking the temperature dependence of a glass [8]. The structural transition $\beta \rightarrow \beta'$ is also evidenced in the thermal conductivity curves by a sudden decrease near 175 K owing to enhanced disorder in the β' structure compared with the β structure.

Figure 4-C depicts the temperature evolution of ZT in this series of compounds. The $\beta \rightarrow \beta'$ structural transition is perceivable around 175 K for all compositions. Owing to compensation effects between the electrical and thermal transport properties, the ZT values appear to vary negligibly with x within experimental uncertainty. A peak ZT value of 0.22 at 300 K is obtained concomitantly for $x = 0.015, 0.025$ and 0.035 . Yet, the anisotropy of the transport properties is however not compensated in ZT giving rise to higher values by 25 % in the perpendicular direction with respect to the parallel direction. Interestingly, all the Bi-substituted compounds show ZT values very similar to those obtained in the Sn-doped compounds [7], suggesting that similar thermoelectric performances may emerge at higher temperatures (*i.e.* $ZT > 0.6$).

Conclusion

We reported on the low-temperature thermoelectric properties of polycrystalline samples of $\beta\text{-As}_{2-x}\text{Bi}_x\text{Te}_3$ for $x = 0.0, 0.015, 0.025$ and 0.035 . Similar ZT values of 0.22 were obtained at 300 K for all the Bi-substituted samples. Remarkably, these values are similar to those unveiled in the Sn-doped compounds suggesting that high ZT values could be achieved above 400 K . Concomitantly, As substitution in the Bi_2Te_3 system remains so far scarcely studied and should be evaluated in relation to the present results on Bi substituted $\beta\text{-As}_2\text{Te}_3$ phases. In the same manner as in the Bi_2Te_3 system, the influence of several substitutions and the thermoelectric performances of other solid solutions based on $\beta\text{-As}_2\text{Te}_3$ are still to be investigated to fully assess its potential as a thermoelectric material for room- or mid-range temperature applications.

Figure and table captions

Fig 1: A) Powder X-Ray diffraction pattern of $\beta\text{-As}_{1.975}\text{Bi}_{0.025}\text{Te}_3$. The observed data are marked as open red circles. The calculated profile is represented by a solid black line while the difference between experimental and numerical patterns is shown by the solid blue line ($\text{RF} = 4.024, \chi^2 = 8.04$). The positions of the Bragg reflections are indicated as green bars. The peak ascribed to AsTe impurity is marked by a black open square. B) Evolution of the hexagonal lattice parameters a and c (respectively blue circles and red squares) as a function of the Bi content. For information, the cell volume (orange diamonds) and the c/a ratio (green triangles) are also represented. C) Perspective view of the hexagonal crystal structure $\beta\text{-As}_2\text{Te}_3$ (the As atoms are represented as small red balls and the Te atoms by large blue balls).

Fig 2: Scanning Electron Microscope (SEM) elemental contrast picture of the sample $\beta\text{-As}_{1.965}\text{Bi}_{0.035}\text{Te}_3$ in Back Scattering Electrons (BSE), together with the corresponding element mapping of As, Bi and Te. The distribution of the elements is overall homogeneous.

Fig 3: Temperature dependence of the electrical resistivity ρ A) and the thermopower B) of the polycrystalline $\beta\text{-As}_{2-x}\text{Bi}_x\text{Te}_3$ samples. The measurements performed parallel and perpendicular to the pressing direction are represented by filled and open symbols respectively. The composition color code is identical in both panels

Fig 4: Temperature dependence of the total thermal conductivity λ A) , the lattice thermal conductivity B) and of the dimensionless figure of merit ZT C) of the polycrystalline $\beta\text{-As}_{2-x}\text{Bi}_x\text{Te}_3$ samples. The measurements

performed parallel and perpendicular to the pressing direction are represented by filled and open symbols respectively. The composition color code is identical in both panels. It is likely that the thermal conductivity above 200 K is overestimated due to radiation issues., hence leading to a slight under estimation of ZT.

Table 1: Hall carrier concentrations (p) and mobility (μ), in the system β -As_{2-x}Bi_xTe₃.at 300K deduced from samples measured perpendicular to the pressing direction.

x	0	0.015	0.025	0.035
p (10^{19} cm^{-3})	8.4	7.1	6.8	8.0
μ ($\text{cm}^2 \cdot \text{V}^{-1} \cdot \text{s}^{-1}$)	48.6	81.2	69.5	57.8

References

1. D.M. Rowe: *Thermoelectrics handbook: macro to nano*. (CRC press, 2006).
2. H. J. Goldsmid: *Thermoelectric refrigeration*. (1964).
3. J. Snyder and E. Toberer, *Nature Mater.* 2008, vol. 7, pp. 105-114.
4. V.G. Yakushev and V.A. Kirinsky, In *DOKLADY AKAD NAUK SSSR*, (1969), pp 882-884.
5. H.W. Shu, S. Jaulmes and J. Flahaut, *Mater. Res. Bull.* 1986, vol. 21, pp. 1509-1514.
6. H.W. Shu, S. Jaulmes and J. Flahaut, *J. Solid State Chem.* 1988, vol. 74, pp. 277-286.
7. J.B. Vaney, J. Carreaud, G. Delaizir, A. Pradel, A. Piarristeguy, C. Morin, E. Alleno, J. Monnier, A.P. Gonçalves, C. Candolfi, A. Dauscher and B. Lenoir, *Adv. Electron. Mater.* 2015, vol. 1, p. 1400008.
8. A.J. Minnich, *Nature Nanotech.* 2013, vol. 8, pp. 392-393.

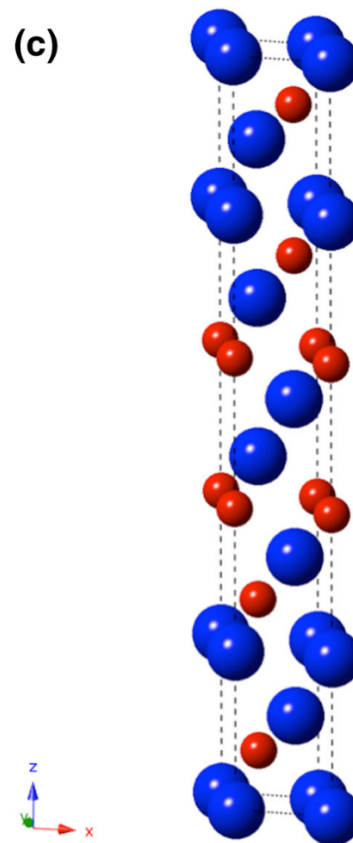
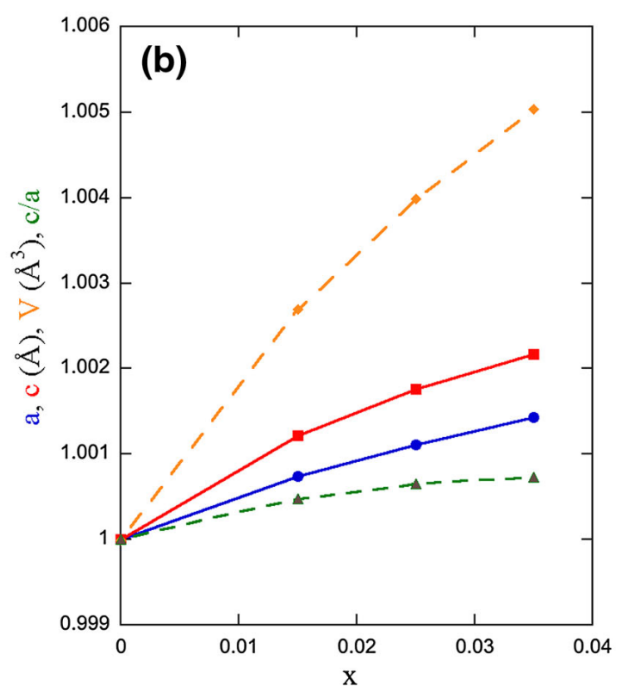
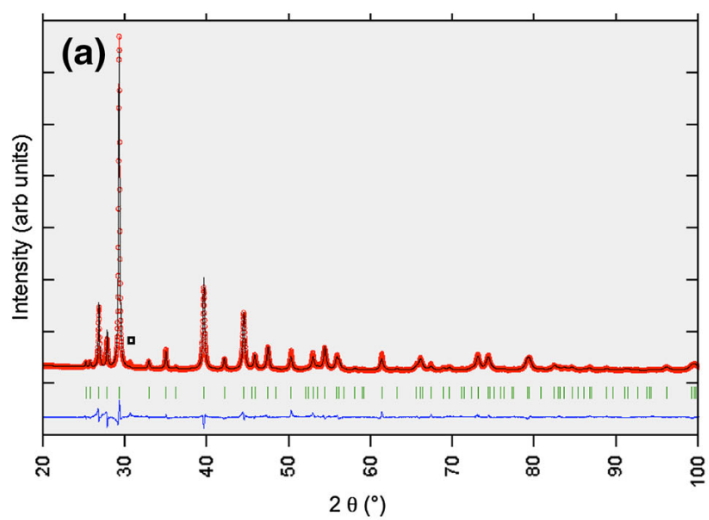


Figure 1

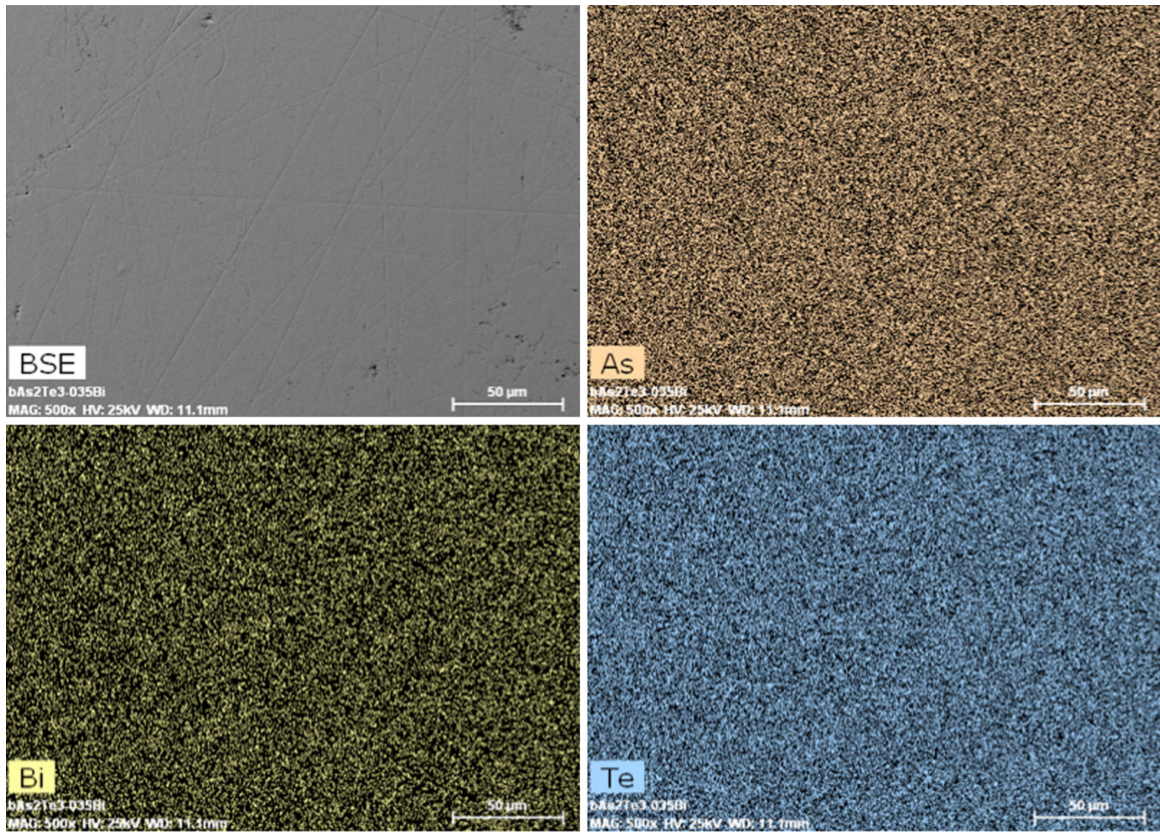


Figure 2

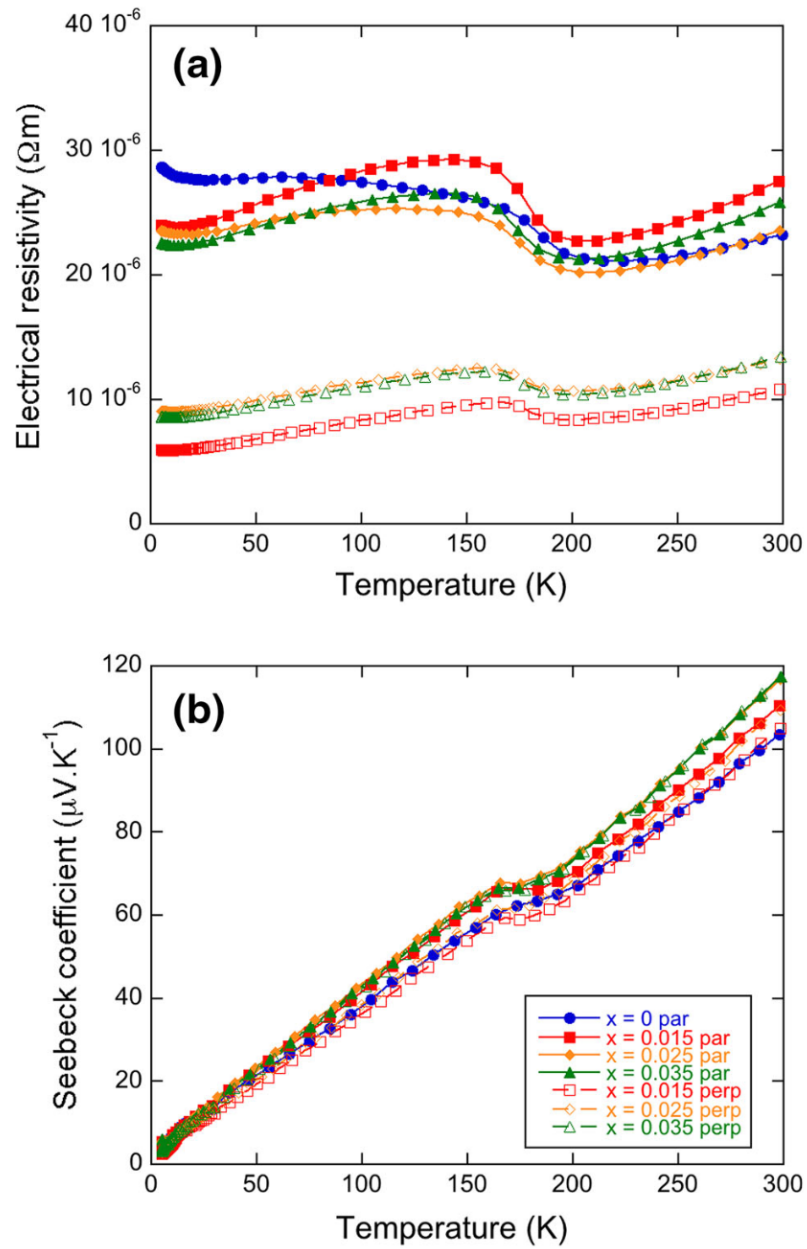


Figure 3

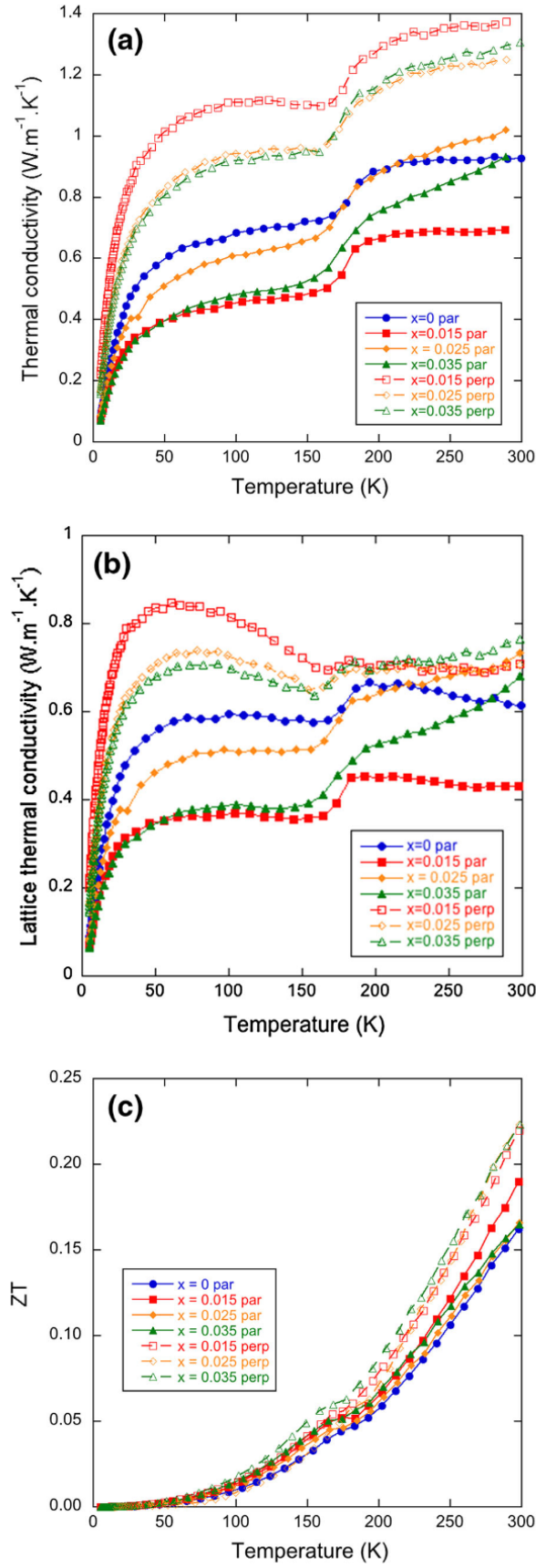


Figure 4